THE JOURNAL OF PROSTHETIC DENTISTRY

RESEARCH AND EDUCATION

# Effects of print orientation and artificial aging on the flexural strength and flexural modulus of 3D printed restorative resin materials

Shaymaa Mudhaffer,[a] Julfikar Haider,[b] Julian Satterthwaite,[c] and Nick Silikas[d]

## ABSTRACT

**Statement of problem.** The integration of computer-aided design and computer-aided manufacture (CAD-CAM) technology has revolutionized restorative dentistry, offering both additive and subtractive manufacturing methods. Despite extensive research on 3-dimensionally (3D) printed materials, uncertainties remain regarding the impact of print orientation on their mechanical properties, especially for definitive resin materials, necessitating further investigation to ensure clinical efficacy.

**Purpose.** The purpose of this in vitro study was to investigate the influence of print orientation and artificial aging on the flexural strength (FS) and flexural modulus (FM) of 3D printed resin materials indicated for definitive and interim restorations.

**Material and methods.** Specimens (2×2×25 mm) were additively manufactured in 3 orientations (0, 45, and 90 degrees) using five 3D printed resins: VarseoSmile Crownplus (VCP), Crowntec (CT), Nextdent CB MFH (ND), Dima CB temp (DT), and GC temp print (GC). A DLP 3D printer (ASIGA MAX UV) was used with postprocessing parameters as per the manufacturer recommendations. FS and FM were tested after storage in distilled water (DW) and artificial saliva (AS) for 24 hours, 1 month, and 3 months at 37 °C. Additional 2×2×16-mm specimens printed at 90 degrees were compared with the milled materials Lava Ultimate (LU) and Telio CAD (TC) after 24 hours of storage in AS at 37 °C (n=10). Measurements were conducted using a universal testing machine (Z020; Zwick/Roell) following the International Organization for Standardization (ISO) 4049 standard. Multiple way ANOVA, 1-way ANOVA, and Tukey HSD post hoc tests (α=.05) were used to analyze the data.

**Results.** Print orientation significantly influenced the FS and FM of 3D printed resin materials, with the 90-degree orientation exhibiting superior mechanical properties ($P<.05$). Definitive resins (CT and VCP) exhibited higher FS and FM compared with interim resins (ND, DT, GC) at all time points ($P<.001$). LU had significantly higher FS and FM compared with other resins ($P<.001$), while TC had similar FS to definitive 3D printed resins. Aging time and media influenced FS and FM, with varying effects observed across different materials and time points. Strong positive correlations were found between filler weight and both FS (r=.83, $P=.019$) and FM. All materials met the minimum FS requirement of 80 MPa (ISO 4049) when printed at 90 degrees.

**Conclusions.** The 90-degree orientation produced specimens with higher FS than 0- and 45-degree orientations. CT recommended for definitive restorations displayed higher FS compared with VCP and those intended for interim use after 3 months of aging. LU exhibited higher FS and FM than 3D printed resins, while TC had similar FS and FM to the latter. Aging effects on 3D printed resins were minimal and were material specific. (J Prosthet Dent xxxx;xxx:xxx-xxx)

Supported by the Saudi Arabian Cultural Bureau (full-time scholarship; recipient: S.M.), London, England, United Kingdom; the funder had no role in study design, data collection and analysis, decision to publish, or preparation of the manuscript.
The authors declare that they have no conflicts of interest related to the publication of this research.
[a]Division of Dentistry, School of Medical Sciences, University of Manchester, Manchester, England, UK.
[b]Department of Engineering, Manchester Metropolitan University, Manchester, England, UK.
[c]Division of Dentistry, School of Medical Sciences, University of Manchester, Manchester, England, UK.
[d]Full Professor, Division of Dentistry, School of Medical Sciences, University of Manchester, Manchester, England, UK.

## Clinical Implications

The highest mean flexural strength values of 3D printed resins for fixed partial dentures were obtained by printing them vertically at a 90-degree angle to the build platform and by using 3D printed resins with high filler loading. The 3D printed definitive resins for fixed partial dentures performed similarly to the milled resins for interim restorations.

The implementation of computer-aided design and computer-aided manufacture (CAD-CAM) technology has significantly influenced restorative dentistry,[1] offering both additive manufacturing (AM) and subtractive manufacturing (SM) methods. SM has been popular in dentistry, involving the milling of solid materials. However, SM has limitations, including material waste, tool wear, accuracy constraints related to complex objects, and potential surface defects.[2,3]

In contrast, AM, or 3D printing, creates 3-dimensional (3D) objects layer by layer, allowing for the rapid production of custom prostheses, with minimal material waste and without tool wear,[1] leading to its increased popularity in dentistry as an alternative to SM.[4–6] VAT polymerization, including stereolithography (SLA) and digital light processing (DLP), is a commonly used AM technology in dentistry, where a light source polymerizes and solidifies photocurable polymers.[7] In SLA, an ultraviolet (UV) laser beam is used, while DLP uses a digital projector screen.[8] Three-dimensionally printed resins are used for surgical guides,[9] complete dentures,[10,11] occlusal devices,[12] as well as interim and, more recently, definitive dental restorations.[13–16]

The mechanical properties of 3D printed restorations are influenced by the material and the manufacturing process.[1,17,18] While the printing process is typically automated with preset parameters including printing velocity and laser intensity and speed, certain preprocessing parameters must be adjusted to achieve optimal outcomes. These include the build orientation, position on the build platform, support structures, and print layer thickness.[1,18,19] Postprocessing stages, such as washing and final polymerization, can also be adjusted and may affect the mechanical properties of the fabricated parts.[20–23] Most materials come with recommended pre- and postprocessing settings, but not all manufacturers provide guidance on the recommended print orientation, a parameter that influences print time, packing density, material consumption, accuracy, and mechanical strength.[1,3,24–27] The 3D printed parts are mechanically anisotropic, meaning mechanical properties can vary with different printing directions.[28] Therefore, understanding the effects of print orientation on mechanical properties is essential for assessing restoration performance. However, published data on the impact of printing orientation on the mechanical properties of 3D printed restorative resin materials are conflicting, leaving uncertainty about which orientation yields favorable mechanical properties.[1,18,19,24,29,30]

While extensive research has been conducted on the mechanical properties of 3D printed interim resin restorative materials,[3,16,19,24,31–35] studies examining the mechanical properties of 3D printed definitive resin materials are sparse,[15,36–38] and some lack important information about the different printing parameters including orientation.[13,39–43]

The mechanical properties of composite resins are also influenced by factors such as the resin matrix,[44] filler load and morphology,[45–47] and the resulting features of the polymer network.[48] In wet environments, composite resins react through water sorption, water solubility, and filler particle exfoliation, affecting their strength.[49–53] Therefore, it is essential to investigate their behavior after artificial aging for clinically relevant testing.

The aim of this in vitro study was to evaluate the effect of print orientation on the flexural strength (FS) and flexural modulus (FM) of 3D printed composite resin materials indicated for definitive and interim restorations after aging in distilled water (DW) and artificial saliva (AS).

The null hypotheses were that no difference would exist in FS and FM between the different print orientations (0, 45 and 90 degrees) of 3D printed resins after aging in DW and AS, between the interim and definitive 3D printed resins after aging for 3 months in DW and AS, between the 3D printed and milled materials after storage in AS for 24 hours, and between the different storage durations (24 hours, 1 month, 3 months) and storage media (DW and AS) regarding the FS of the investigated 3D printed materials.

## MATERIAL AND METHODS

Five resin materials for additive manufacturing and 2 for subtractive manufacturing were used in this study (Table 1). Specimens for the AM group were printed in 3 orientations (0, 45, and 90 degrees) with dimensions of 2×2×25 mm (N=180/material, 60/orientation). Measurements were recorded at 24 hours, 1 month, and 3 months after aging in DW and AS at 37 °C (n=10). Additional 2×2×16-mm specimens were printed with a 90-degree orientation. FS measurements for these, in addition to the milled group, were recorded after 24 hours of storage in AS at 37 °C (n=10). The dimensions of the second set of specimens were dictated by the size restrictions of the milled blocks. The sample size (n=10)

Table 1. Manufacturers' composition information for investigated materials

| | Material | Code | Manufacturer | Composition | wt% | Lot. # | Shade | Indications |
|---|---|---|---|---|---|---|---|---|
| 3D printed | Varseosmile Crown$^{plus}$ | VCP | BEGO | Esterification products of 4.4′-isopropylidiphenol, ethoxylated and 2-methylprop−2enoic acid | 5–75 | 600414 | A2 | Definitive crowns, inlays, onlays, and veneers |
| | | | | Silanized dental glass (particle size 0.7 µm) | 30–50 | | | |
| | | | | Diphenyl (2,4,6-trimethylbenzoyl) phosphine oxide | <2.5 | | | |
| | | | | Methyl benzoylformate | - | | | |
| | Crowntec | CT | Saremco Dental AG | Bis-EMA | 50–75 | D937 | A2 | Definitive crowns, inlays, onlays, veneers, denture teeth and interim fixed partial dentures |
| | | | | Trimethylbenzonyldiphenyl phosphine oxide | 0.1 - <1 | | | |
| | | | | Silanized dental glass, pyrogenic silica (particle size 0.7 µm) | 30–50 | | | |
| | NextDent C B MFH | ND | 3D systems | 7,7,9(or 7,9,9)-trimethyl−4,13-dioxo−3,14-dioxa−5,12-diazahexadecane−1,16-diyl bismethacrylate | 50–75 | WX495N02 | N1 | Crowns and fixed partial dentures for long term interim use |
| | | | | 2-hydroxyethyl methacrylate *(HEMA)* | <25 | | | |
| | | | | Ethoxylated bisphenol A dimethacrylate | <10 | | | |
| | | | | Ethylene dimethacrylate | <10 | | | |
| | | | | Silicon dioxide | 1–5 | | | |
| | | | | Diphenyl (2,4,6-trimethylbenzoyl) phosphine oxide | 1–5 | | | |
| | | | | Mequinol; 4-methoxyphenol; hydroquinone monomethyl ether | <0.1 | | | |
| | | | | Titanium dioxide | <0.1 | | | |
| | Dima CB temp | DT | Kulzer GmbH | Esterification products of 4,4′-isopropylidiphenol, ethoxylated and 2-methylprop−2enoic acid | 40–60 | CD21G06A35 | A2 | Interim crowns and fixed partial dentures up to 1 year |
| | | | | 7,7,9(or 7,9,9)-trimethyl−4,13-dioxo−3,14-dioxa−5,12-diazahexadecane−1,16-diyl bismethacrylate | 30–50 | | | |
| | | | | Propylidynetrimethyl trimethacrylate | 3–10 | | | |
| | | | | Diphenyl (2,4,6-trimethylbenzoyl) phosphine oxide | <3 | | | |
| | | | | Mequinol | <1 | | | |
| | GC temp print | GC | GC dental | UDMA | 50–75 | 2206101 | A2 | Long term interim crowns, fixed partial dentures, inlays, onlays, and veneers |
| | | | | *2,2′-ethylenedioxydiethyl dimethacrylate* | 10- <25 | | | |
| | | | | Esterification products of 4,4′-isopropylidenediphenol, ethoxylated and 2-methylprop2-enoic acid | 2.5- <5 | | | |
| | | | | Silicon dioxide (quartz) | 10- <25 | | | |
| | | | | Diphenyl (2,4,6-trimethylbenzoyl) phosphine oxide | <2.5 | | | |
| | | | | 2-(2 H-benzotriazol−2-yl)-p-cresol | 0.1-<0.2 | | | |
| Milled | Lava Ultimate | LU | 3 M ESPE | BisGMA, UDMA, BisEMA, TEGDMA | 20 | NC95259 | A2 | Definitive inlays, onlays, and veneers |
| | | | | Silica nanomers (20 nm)Zirconia nanomers (4- 11 nm)Silica-zirconia nanoclusters (0.6–10 µm) | 80 | | | |
| | Telio CAD | TC | Ivoclar AG | Polymethyl methacrylate | 99.5 | Z02TYX | A2 | Interim crowns, interim fixed partial dentures, and implant-supported interim crowns |
| | | | | Pigments | <1 | | | |

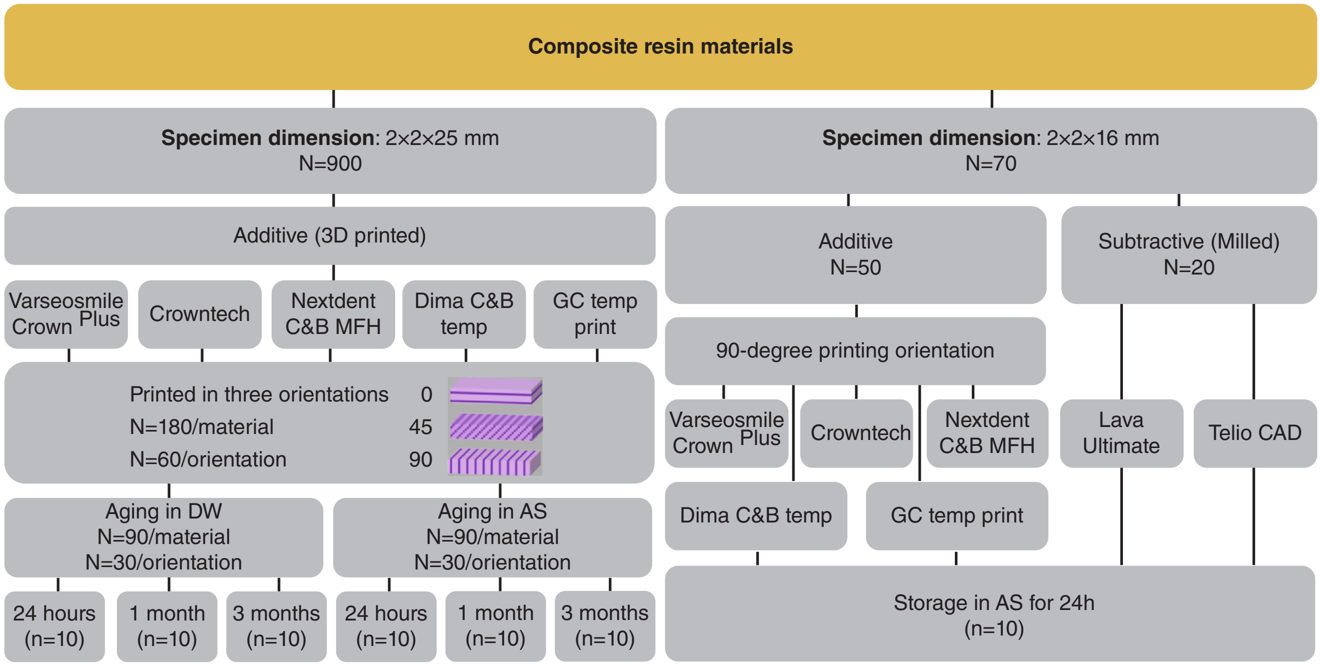


**Figure 1.** Study design of additive and subtractive resin materials.

was based on previous studies,[1,54] and all specimens were allocated to their designated storage media/time using a simple computer randomization (IBM SPSS Statistics, v29.0; IBM Corp). The study design is described in Figure 1.

One specimen (2×2×25 mm) was designed using an online software program (Tinkercad), saved as a standard tessellation language (STL) file, and imported into the CAM software program (Composer version 1.3.2, 2021; ASIGA). The print parameters were then selected; these included print orientation (0, 45, and 90 degrees) (Fig. 2A), specimen number (n=10/orientation), layer thickness (50 µm), and support design (automatically generated). Specimens were printed using an open system 3D printer (ASIGA MAX UV; ASIGA) that uses DLP technology and operates at a light wavelength of 385 nm.

The specimens were divided into 3 subgroups according to orientation. The 0-degree specimens were printed horizontally, perpendicular to the load direction; the 45-degree specimens were printed with an angle; and the 90-degree specimens were printed vertically, parallel to the load direction (Fig. 2B).

After printing, the specimens were cleaned in an automated wash device (Form Wash; Formlabs Inc) using an alcohol solution (96% ethanol; Sigma Aldrich) for 5-minutes to eliminate residual surface monomers. Supports were removed with a scalpel, and the specimens were postpolymerized following the manufacturers' recommendation for each material (Table 2) and manually abraded with a 320-grit silicon carbide paper (Metaserv 250 Grinder Polisher; Buehler Co) to remove any flash and smooth the edges. The dimensions of specimens were confirmed using digital calipers (PDC150M; Draper tools Ltd) following the International Organization for Standardization (ISO) 4049 standard.[55] Following postpolymerization, a noticeable bend was observed along the length of the specimens printed at 0-degrees, likely linked to polymerization shrinkage. This bend was absent in specimens printed at other orientations. A pilot study was therefore conducted to determine the most appropriate side for applying the force during flexural testing, and testing proceeded with the bend facing the applied force.

Specimens of subtractive CAD-CAM blocks were sectioned using a diamond blade (MK 303; MK Diamond) mounted on a saw (Isomet 1000 Precision Saw; Buehler Co) under constant water irrigation and then polished similarly to the 3D printed group. The dimensions (2×2×16 mm) were confirmed using digital calipers to an accuracy of ±0.01 mm.

The inorganic filler content was determined by eliminating the organic component through a heating process known as the Ash technique (ISO 1172, 1999).[56] Disk specimens (Ø12×2 mm) were printed in a 0-degree orientation (n=3), placed on a ceramic crucible, and heated in an electric furnace (Programat EP 5000; Ivoclar AG) to a temperature of 600 °C for 30 minutes. The specimens were weighed using an electronic scale with an accuracy of ±0.01 mg (Ohaus Analytical Plus; Ohaus Corp). The percentage of inorganic filler weight was calculated from:

$$\textit{Filler weight}.\ \% = \frac{(w_3 - w_1)}{(w_2 - w_1)} \times 100,$$

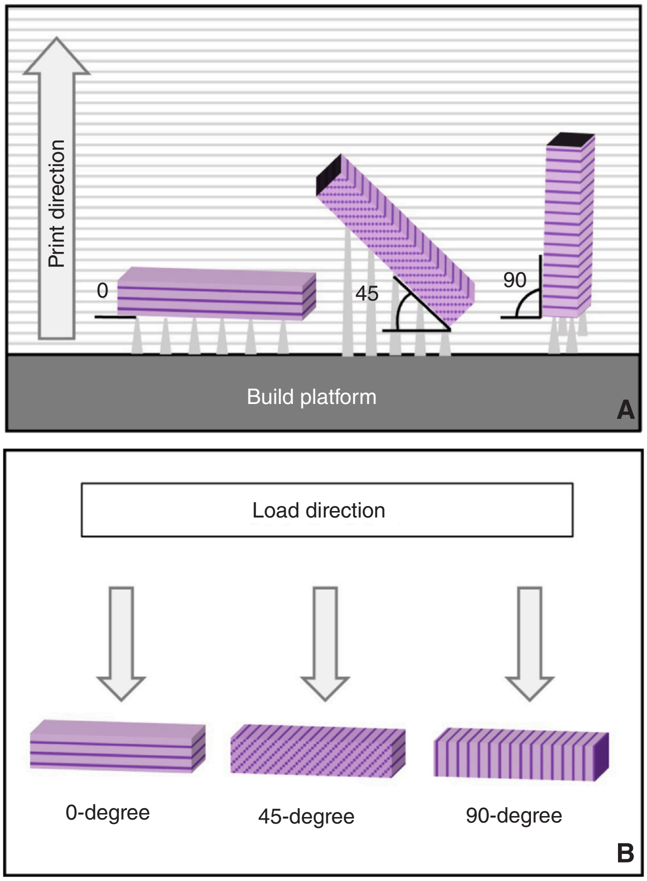


**Figure 2.** A, Schematic representation of print design of bar-shaped specimens in 0, 45, and 90-degree print orientations. B, Direction of force on specimen surface during flexural strength test with respect to layer orientations.

where $w_1$ is the initial mass of the dry crucible, $w_2$ is the initial mass of dry crucible combined with the dried specimen, and $w_3$ is the final mass of the crucible combined with the specimen residue.

To simulate chemical degradation, all specimens were placed inside glass vials filled with either DW or AS[57,58] and placed in a $CO_2$ incubator (function line BB 16; Heraeus Instruments) at 37 °C. The AS solution was prepared by dissolving sodium chloride (0.4 g), potassium chloride (0.4 g), calcium chloride (0.795 g), sodium dihydrogen phosphate (0.69 g), and sodium sulfide hydrate (0.005 g) in 1000 mL of distilled water.[59,60] The pH of AS was 5.52 as determined by a digital microprocessor pH meter (DELTA 340; Mettler Toledo Ltd).

Flexure testing has been recommended for evaluating dental composite resin, as it assesses the ability of the fixed dental prosthesis to resist plastic deformation when subjected to loads.[61] A universal testing machine (Z020; Zwick/Roell) with a 500-N cell load was used for the measurements. Each specimen was placed on 2 supporting rods mounted parallel with either a 20-mm (± 0.1) (for the 25 mm specimens) or a 12-mm (± 0.1) (for the 16-mm specimens) distance between them, with the third loading rod centered midway between the 2 supports. All specimens were subjected to a 3-point bend test under increasing load at a crosshead speed of 1 mm/minute until fracture as specified by the ISO 4049[55] and 10477 standards.[62] The flexural strength (MPa) was calculated from:

$$\sigma = 3Fl/(2bh^2),$$

where F is the maximum load exerted on the specimen (N), l is the distance between the supports, b is the width of the specimen before water storage, and h is the height of the specimen before water storage (all mm). The flexural modulus was calculated from a tangent to the initial slope of the stress/strain curve.

One fractured specimen from each orientation was mounted on an aluminum stub, coated with gold, and examined with a scanning electron microscope (SEM) (JSM-6610 LV; JOEL Co). Images were captured at magnifications ranging from ×500 (to assess for layer homogeneity) to ×20 000 (to assess for resin matrix or filler degradation) using a secondary electron detector with an acceleration voltage of 10.0 kV.

The data were analyzed using a statistical software program (IBM SPSS Statistics, v29.0; IBM Corp). The results were tested for normal distribution and homogeneity of variance using the Shapiro-Wilk and Levene tests respectively. Multiple-way analysis of variance was performed to investigate the interactions between material group, build orientation, aging time, and aging media. Data within each measurement parameter were analyzed with 1-way ANOVA and a Tukey post hoc test. The $t$ test was performed to investigate the difference

**Table 2.** Postpolymerization device parameters provided by their manufacturers

| | Postpolymerization Device | | |
|---|---|---|---|
| | **Form Cure** | **Otoflash G171** | **Cara Print LED Cure** |
| Manufacturer | Formlabs | NK-Optik | Kulzer GmbH |
| Technology | Ultraviolet light (UV) | Flashlight | Light-emitting diode (LED) |
| Number of light sources | 13 | 2 | 10 |
| Light intensity | 39 Watt | 200 Watt | 15–150 W |
| Light spectrum (wavelength) | 405 nm | 280–700 nm (peak 400–500 nm) | 370–470 nm (peak 397–450 nm) |
| Maximum temperature | 60–80 °C | n/a | 30–80 °C |
| Materials and post-polymerization recommendation | Nextdent CB MFH (60 °C for 30 min) | Varseosmile Crown$^{plus}$ (2×1500 flashes)<br>Crowntec (2×2000 flashes)<br>GC Temp Print (2×400 flashes) | Dima CB Temp (60 °C for 20 min) |

**Table 3.** Mean ±standard deviation values for filler content wt% of all studied materials measured using ash method (n=3)

| Category | Material | Manufacturer Filler wt% | Measured Filler (Residue) wt% |
|---|---|---|---|
| Subtractive | LU | 80 | 73.5 ±1.3$^{A}$ |
| | TC | N/A | N/A |
| Additive | VCP | 30–50 | 33.8 ±0.3$^{B}$ |
| | CT | 30–50 | 33.4 ±1.9$^{B}$ |
| | ND | Not disclosed | 7.4 ±0.1$^{D}$ |
| | DT | Not disclosed | 0.95 ±0.1$^{E}$ |
| | GC | 10–25 | 19.5 ±0.1$^{C}$ |

Different superscript letters denote significant variations between materials (P<.05).

between the aging media. Pearson correlation analysis was conducted to examine the relationship between filler weight and FS and FM (α=.05 for all tests).

## RESULTS

Filler wt% (Table 3) was found to be statistically different in the following sequence: LU > CT ≥ VCP > GC > ND > DT (*P*<.05). The filler wt% of VCP and CT were similar (*P*=.9). TC is a PMMA material and does not contain any fillers.

Means and standard deviations for the FS and FM of the 3D printed resins are listed in Tables 4 and 5. The results indicated a significant main effect for material, print orientation, aging media, and aging time on FS and FM (*P*<.001). The parameter material exerted the highest influence on FS and FM (FS: $\eta_p^2$=.67, FM: $\eta_p^2$=.98) followed by the print orientation (FS: $\eta_p^2$=.46, FM: $\eta_p^2$=.34), aging time (FS: $\eta_p^2$=.15, FM: $\eta_p^2$=.14), and aging media (FS: $\eta_p^2$=.08, FM: $\eta_p^2$=.21). The interaction between the

**Table 4.** Means ±standard deviations (MPa) for flexural strength of AM resins printed with three orientations (0, 45, and 90 degrees) and 2×2×25-mm specimen dimension after aging in distilled water and artificial saliva for 24 h, 1 m, and 3 m at 37 °C (n=10)

| Category | Material | Orientation (Degrees) | Distilled Water | | | Artificial Saliva | | |
|---|---|---|---|---|---|---|---|---|
| | | | 24 h | 1 m | 3 m | 24 h | 1 m | 3 m |
| Definitive | VCP | 0 | 87.3 ±3.7$^{a1}$ | 75.4 ±15.8$^{a1}$ | 84.6 ±9.9$^{a1}$ | 95.8 ±5.7$^{a1}$ | 64.0 ±3.9$^{a2}$ | 69.1 ±9.2$^{a2}$ |
| | | 45 | 100.7 ±5.0$^{b1}$ | 83.8 ±8.5$^{a2}$ | 93.8 ±10.5$^{ab3}$ | 86.1 ±7.1$^{b1}$ | 85.8 ±9.9$^{b1}$ | 86.4 ±7.2$^{b1}$ |
| | | 90 | 101.8 ±8.8$^{b1}$ | 98.9 ±7.2$^{b2}$ | 96.6 ±8.1$^{b2}$ | 103.2 ±8.3$^{a1}$ | 99.8 ±5.8$^{c1}$ | 100.5 ±6.7$^{c1}$ |
| | CT | 0 | 102.3 ±9.2$^{a1}$ | 100.2 ±9.8$^{a1}$ | 94.4 ±13.4$^{a1}$ | 111.9 ±8.8$^{a1}$ | 81.0 ±11.6$^{a2}$ | 88.6 ±9.7$^{a2}$ |
| | | 45 | 113.2 ±8.9$^{a1}$ | 113.2 ±9.7$^{b1}$ | 103.1 ±9.1$^{ab1}$ | 112.2 ±7.3$^{b1}$ | 95.6 ±6.8$^{b2}$ | 93.3 ±6.9$^{a2}$ |
| | | 90 | 125.9 ±11.5$^{b1*}$ | 121.3 ±9.5$^{b1}$ | 113.8 ±5.6$^{b1}$ | 115.9 ±5.5$^{c1*}$ | 116.9 ±9.4$^{c1}$ | 115.9 ±6.9$^{b1}$ |
| Interim | ND | 0 | 90.5 ±4.1$^{a1}$ | 81.8 ±3.6$^{a2}$ | 87.6 ±4.8$^{a3}$ | 87.7 ±2.7$^{a1}$ | 72.9 ±1.4$^{a2}$ | 81.2 ±3.5$^{a3}$ |
| | | 45 | 102.6 ±5.6$^{b1}$ | 83.6 ±1.5$^{a2}$ | 89.6 ±1.7$^{a3}$ | 94.3 ±2.1$^{b1}$ | 77.5 ±1.2$^{b2}$ | 86.6 ±3.81$^{b3}$ |
| | | 90 | 106.2 ±4.9$^{b1*}$ | 83.2 ±1.5$^{a2*}$ | 89.9 ±1.9$^{a2}$ | 95.5 ±3.2$^{b1*}$ | 79.9 ±1.4$^{c2*}$ | 91.3 ±2.1$^{c3}$ |
| | DT | 0 | 79.6 ±3.0$^{a1}$ | 78.3 ±8.6$^{a1}$ | 79.4 ±5.7$^{a1}$ | 80.4 ±2.2$^{a1}$ | 79.5 ±2.2$^{a1}$ | 78.1 ±7.0$^{a1}$ |
| | | 45 | 81.7 ±2.4$^{a1}$ | 87.5 ±10.0$^{b2}$ | 92.1 ±3.8$^{b2}$ | 80.0 ±4.2$^{a1}$ | 79.2 ±3.2$^{a1}$ | 87.7 ±3.2$^{ab2}$ |
| | | 90 | 87.7 ±2.1$^{b1}$ | 102.0 ±1.2$^{c2*}$ | 93.4 ±6.9$^{b3}$ | 86.8 ±1.1$^{b1}$ | 86.6 ±3.4$^{b1*}$ | 93.3 ±1.7$^{b2}$ |
| | GC | 0 | 69.4 ±3.5$^{a1}$ | 82.6 ±3.3$^{a2}$ | 88.8 ±7.2$^{a2}$ | 74.4 ±4.0$^{a1}$ | 78.7 ±8.3$^{ab1}$ | 87.4 ±8.6$^{a2}$ |
| | | 45 | 74.9 ±3.3$^{b1}$ | 76.8 ±4.9$^{b1*}$ | 79.7 ±5.6$^{b1}$ | 85.4 ±5.5$^{b1}$ | 75.4 ±3.3$^{a2*}$ | 76.9 ±9.5$^{b2}$ |
| | | 90 | 82.4 ±3.4$^{c1}$ | 90.3 ±3.8$^{c2}$ | 89.7 ±5.8$^{a2}$ | 85.2 ±3.8$^{b1}$ | 82.9 ±4.3$^{a1}$ | 89.2 ±6.9$^{a2}$ |

Values marked with same superscript letter or number not significantly different from each other (P>.05).

a,b,c Describe significant differences between orientations within one 3D printed material and aging level. 1,2,3 Describe significant differences between aging levels within one material and aging media. * Indicates significant difference between aging media for same aging level.

**Table 5.** Means ±standard deviations (MPa) for flexural modulus of AM resins printed with three orientations (0, 45, and 90 degrees) and 2×2×25-mm specimen dimension after aging in distilled water and artificial saliva for 24 h, 1 m, and 30 m at 37 °C (n=10)

| Category | Material | Orientation (Degrees) | Distilled Water | | | Artificial Saliva | | |
|---|---|---|---|---|---|---|---|---|
| | | | 24 h | 1 m | 3 m | 24 h | 1 m | 3 m |
| Definitive | VCP | 0 | 2976.1 ±86.9$^{a1}$ | 2965.7 ±75.2$^{a1}$ | 3083.8 ±53.4$^{a2}$ | 2989.9 ±134.3$^{a1}$ | 3013.9 ±80.3$^{a1}$ | 3453.9 ±94.6$^{a2}$ |
| | | 45 | 3668.9 ±58.3$^{b1}$ | 2858.0 ±80.8$^{b2}$ | 3022.7 ±75.9$^{a3}$ | 2907.2 ±58.7$^{b1}$ | 3016.6 ±61.8$^{a1}$ | 3193.8 ±67.4$^{b2}$ |
| | | 90 | 3730.0 ±155.3$^{b1}$ | 3161.4 ±105.8$^{c2}$ | 3102.7 ±168.6$^{a2}$ | 3186.0 ±37.9$^{b1}$ | 3264.4 ±85.2$^{b1}$ | 3565.9 ±72.2$^{c2}$ |
| | CT | 0 | 3357.9 ±215.2$^{a12}$ | 3434.7 ±105.9$^{a1}$ | 3362.5 ±240.1$^{a2}$ | 3328.7 ±98.8$^{a1}$ | 3222.8 ±79.5$^{a1}$ | 3508.8 ±101.7$^{a2}$ |
| | | 45 | 3981.8 ±41.3$^{b1}$ | 3304.1 ±52.7$^{a2}$ | 3165.3 ±131.0$^{b2}$ | 3124.7 ±75.4$^{a1}$ | 3238.5 ±63.2$^{a1}$ | 3402.3 ±76.9$^{a2}$ |
| | | 90 | 3706.6 ±65.0$^{b1*}$ | 3784.8 ±165.1$^{b1}$ | 3104.6 ±65.2$^{ab2}$ | 3181.4 ±63.1$^{a1*}$ | 3360.1 ±99.0$^{b1}$ | 3536.7 ±52.7$^{b2}$ |
| Interim | ND | 0 | 1997.7 ±106.9$^{a1}$ | 2077.6 ±81.7$^{a2}$ | 2107.0 ±67.9$^{ab2}$ | 1779.5 ±50.3$^{a1}$ | 1754.5 ±39.9$^{a1}$ | 2045.4 ±88.7$^{a2}$ |
| | | 45 | 2630.1 ±112.6$^{b1}$ | 1886.5 ±73.4$^{b2}$ | 2063.9 ±117.4$^{a3}$ | 1912.8 ±26.9$^{b1}$ | 1827.1 ±42.5$^{b2}$ | 2062.9 ±94.8$^{a3}$ |
| | | 90 | 2765.7 ±165.8$^{b1*}$ | 1984.2 ±76.4$^{c2*}$ | 2186.1 ±24.8$^{b3}$ | 1925.5 ±71.8$^{b1*}$ | 1862.2 ±34.0$^{b1*}$ | 2196.5 ±51.0$^{b2}$ |
| | DT | 0 | 1575.1 ±62.6$^{a1}$ | 1849.6 ±82.6$^{a2}$ | 1735.6 ±69.4$^{a3}$ | 1667.5 ±81.4$^{a1}$ | 1693.6 ±64.2$^{a1}$ | 1746.8 ±74.0$^{a2}$ |
| | | 45 | 1581.9 ±62.0$^{a1}$ | 1942.1 ±88.4$^{b2}$ | 1772.7 ±34.6$^{a3}$ | 1648.6 ±29.1$^{a1}$ | 1714.0 ±67.4$^{a2}$ | 1773.8 ±44.1$^{a3}$ |
| | | 90 | 1678.5 ±44.1$^{b1}$ | 2098.3 ±40.2$^{c2*}$ | 1793.6 ±56.0$^{a3}$ | 1627.1 ±37.0$^{a1}$ | 1685.7 ±46.8$^{a1*}$ | 1780.4 31.3$^{a2}$ |
| | GC | 0 | 1786.6 ±43.2$^{a1}$ | 2137.8 ±63.1$^{a2}$ | 2310.6 ±111.1$^{a3}$ | 1903.3 ±87.5$^{a1}$ | 2183.9 ±66.3$^{a2}$ | 2377.8 ±69.0$^{a3}$ |
| | | 45 | 1966.1 ±85.7$^{b1}$ | 2125.3 ±105.6$^{a12}$ | 2125.3 ±105.6$^{b2}$ | 2088.9 ±105.7$^{b1}$ | 2054.1 ±61.8$^{b1}$ | 2141.2 ±72.7$^{b1}$ |
| | | 90 | 2017.6 ±86.6$^{b1}$ | 2285.6 ±79.6$^{b2*}$ | 2376.5 ±103.8$^{a2}$ | 2236.3 ±42.3$^{c1}$ | 2159.6 ±104.0$^{a2*}$ | 2356.0 ±66.1$^{a3}$ |

Values marked with same superscript letter or number not significantly different from each other (P>.05).

a,b,c Describe significant differences between orientations within one 3D printed material and aging level. 1,2,3 Describe significant differences between the aging levels within one material and aging media. * Indicates significant difference between aging media for same aging level.

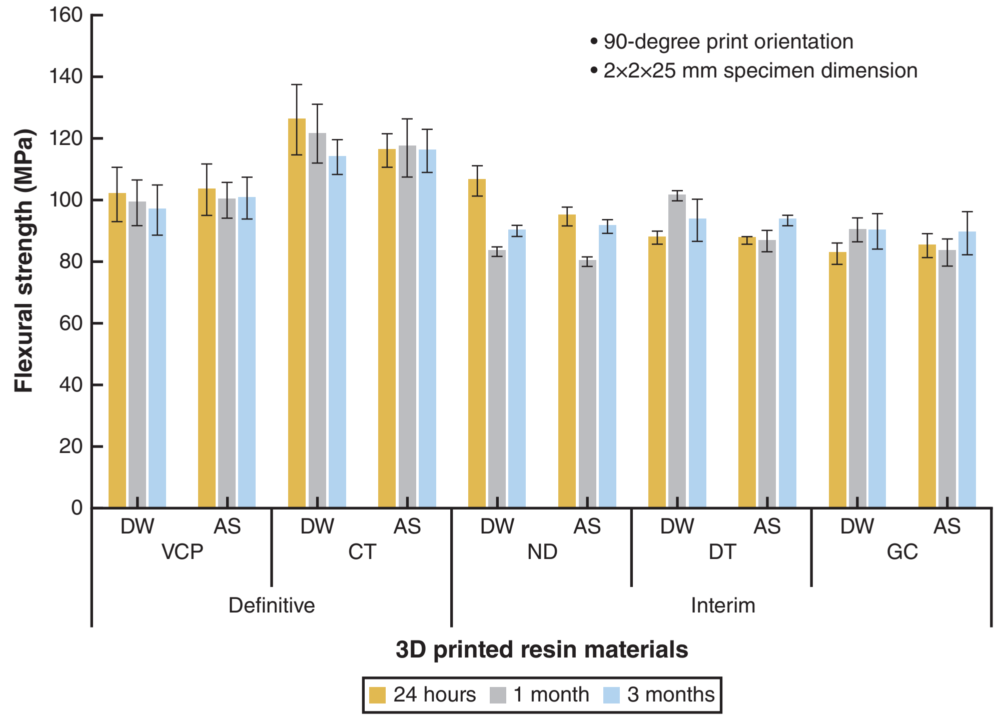


**Figure 3.** Flexural strength of 3-dimensionally printed resin materials (90-degree) with specimen dimension of 2×2×25 mm after aging in distilled water and artificial saliva for 24 h, 1 month, and 3 months.

parameters material and print orientation, material and aging media, and material and aging time were also significant (*P*<.001). A strong positive correlation was found between filler weight and FS (r=.83, *P*=.019) and between filler weight and FM (r=.96, *P*=.001).

Significant differences were found in FS and FM among the 3 orientations for all 3D printed materials (*P*<.05). A trend was observed at 24 hours in the specimens printed at 90-degrees, as they exhibited significantly higher FS and FM than the 0-degree specimens (*P*<.05), while the FS and FM for the 45-degree specimens varied across materials and did not follow a specific trend. However, CT in AS did not show a significant difference in FS between orientations (*P*=.4), and DT in AS did not show any statistical differences in FM between orientations throughout the entire aging period (*P*=.2). Similar trends were observed at 1 month, when the 90-degree specimens maintained the highest FS and FM for all materials, except for ND in DW (*P*=.2). At 3 months, the FS of the 90-degree specimens for all materials remained statistically higher than those of the 0-degree specimens (*P*<.05), except for ND in DW (*P*=.3) and GC in both storage media (*P*=.9). Although the 90-degree specimens had higher FM measurements, the statistical differences varied among orientations.

Since the 90-degree specimens exhibited higher FS than the other orientations, this print orientation was selected for all comparisons of the remaining parameters (materials, aging time, and aging media). Differences were observed in FS and FM between the definitive and interim 3D printed resins (*P*<.001) (Fig. 3). The definitive resin CT exhibited the highest FS and FM, followed by VCP, with a statistical difference in FS between them (*P*<.001) while having similar FM (*P*=.78). The interim 3D printed resins exhibited the lowest FS and FM with statistical differences between some of them initially (*P*<.001), but no statistical differences were found between them after 3 months (*P*≥.204); their FM was significantly different (*P*<.001).

Differences in flexural strength (Fig. 4) and flexural modulus (Table 6) were observed between milled and 3D printed materials (*P*<.001). LU had higher FS and FM compared with all other materials. TC had similar FS to the definitive 3D printed resins (*P*=.9), as well as DT (*P*>.999) and ND (*P*=.05), while having similar FM to the interim 3D printed resins (*P*≥.7).

At 24 hours and 1 month, significant differences were found between DW and AS for all materials except VCP, where FS and FM measurements in DW were higher than those in AS. However, after 3 months, no significant differences were observed between the 2 aging media (Tables 4 and 5).

The behavior of 3D printed materials varied throughout the aging period. For VCP, CT, and ND, the FS decreased after 3 months compared with 24 hours (*P*<.05), although this reduction was not statistically significant for VCP (in both aging media) and CT (in

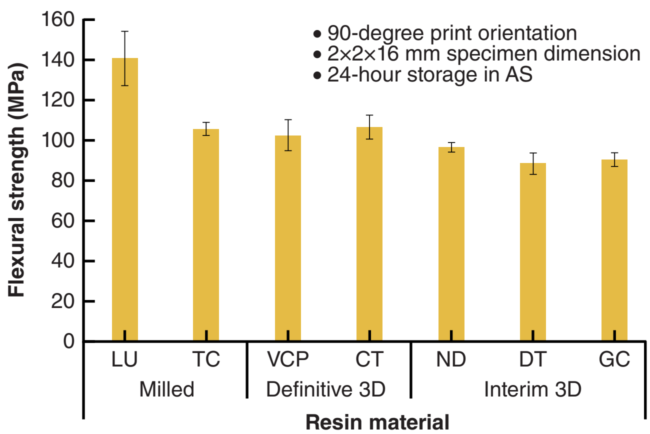


**Figure 4.** Flexural strength of 3-dimensionally printed and milled resin materials with specimen dimension of 2×2×16 mm after storage in artificial saliva for 24 h.

**Table 6.** Mean ±standard deviation (MPa) for flexural strength and flexural modulus of milled and 3D printed resins with 2×2×16-mm specimen dimension after storage in artificial saliva for 24 h at 37 °C (n=10)

| Category | | Material | Flexural Strength | Flexural Modulus |
|---|---|---|---|---|
| Milled | | LU | 139.8 ±13.3[a] | 7874.4 ±628.9[a] |
| | | TC | 105.1 ±3.1[b] | 1626.6 ±98.1[d] |
| 3D printed | Definitive | VCP | 101.8 ±7.6[b] | 2742.7 ±79.9[b] |
| | | CT | 105.8 ±5.9[b] | 3044.3 ±91.7[b] |
| | Interim | ND | 95.9 ±2.4[d] | 1484.8 ±33.4[d] |
| | | DT | 87.9 ±5.3[d] | 1453.9 ±28.6[d] |
| | | GC | 89.9 ±3.3[d] | 1652.4 ±33.8[d] |

Values with same superscript letters in column represent non-significant difference between materials ($P>.05$)

AS). FS for DT and GC (in DW) slightly increased after 3 months compared with 24 hours ($P<.05$). The FM of all materials increased after 3 months compared with 24 hours, except for CT, VCP, and ND in DW, where the FM decreased.

SEM images of 3D printed specimens are shown in Figures 5 and 6. At 24 hours, no discernible 50−μm layering was observed in any of the 3 orientations. At 3 months, all materials exhibited signs of voids resulting from filler detachment, except for DT. Filler particle clustering was prominently observed in the ND and GC specimens. DT images displayed an absence of filler particles and indicated signs of peeling.

## DISCUSSION

Print orientation had a significant impact on the FS and FM of 3D printed resin materials after aging for 3 months. Thus, the null hypothesis that no difference would exist in FS and FM among the different print orientations (0, 45, and 90 degrees) of 3D printed resins was rejected. Significant differences in FS and FM were identified between the definitive and interim 3D printed materials and between the 3D printed and milled materials. Therefore, the null hypotheses that no difference would exist in FS and FM between the interim and definitive 3D printed resins after aging for 3 months in DW and AS and between the 3D printed and milled materials after storage in AS for 24 hours were rejected. Significant differences were identified between storage times and storage media; thus, the null hypothesis that no difference would exist between the different storage durations (24 hours, 1 month, 3 months) and storage media (DW and AS) regarding the FS of the investigated 3D printed materials was rejected.

Within the oral cavity, diverse stresses, including compressive, tensile, and shear, exert pressure on a fixed dental prosthesis, potentially leading to structural failure.[52,53] Therefore, fixed dental prostheses must meet specific standards in their mechanical strength to withstand deformation and fracture under various intraoral forces. According to the ISO 4049 standard,[55] polymer base materials should have a minimum FS of 80 MPa.

In the present study, the force was applied parallel to the layer orientation in the 90-degree printed specimens and perpendicular to the 0-degree printed specimens (Fig. 2B). It was assumed that the 90-degree specimens would result in lower values based on the assumption that the strength between successive layers was weaker than within individual layers.[1,29,30] This assumption was supported by other research findings[19,25] which indicated that the FS of 0-degree specimens exceeded that of 90-degree specimens. However, the present study contradicted these assumptions, revealing that the 90-degree specimens exhibited higher FS and FM than the 0-degree specimens and, occasionally, the 45-degree specimens, consistent with other studies.[17,24,34] These findings could be attributed to the strong adhesion between layers, making strength differences negligible.[10,18,27] The SEM images (Figs. 5 and 6) showed no distinct layers at the fracture sites, confirming homogeneity, consistent with other studies.[10,35] Another factor could be the different degree of conversion during polymerization. Specifically, the 0-degree orientation required 86 layers per specimen, while the 90-degree orientation required 546 layers, resulting in increased light exposure and potentially influencing the degree of conversion.[10] Notably, at the 90-degree orientation, all materials met the minimum FS requirement of 80 MPa (ISO 4049), unlike the 0- and 45-degree orientations for some materials (VCP, GC, DT).

Among the tested 3D printed materials, CT and VCP had the highest filler loads at 33%, followed by GC at 19.45%. ND and DT had lower filler loads, at 7.43% and 0.95%, respectively. Higher filler loads can enhance mechanical properties,[63] explaining why CT and VCP showed greater FS than other materials. Yet, GC, despite its higher filler load than ND and DT, exhibited similar FS but higher FM than ND and DT after 3 months. The

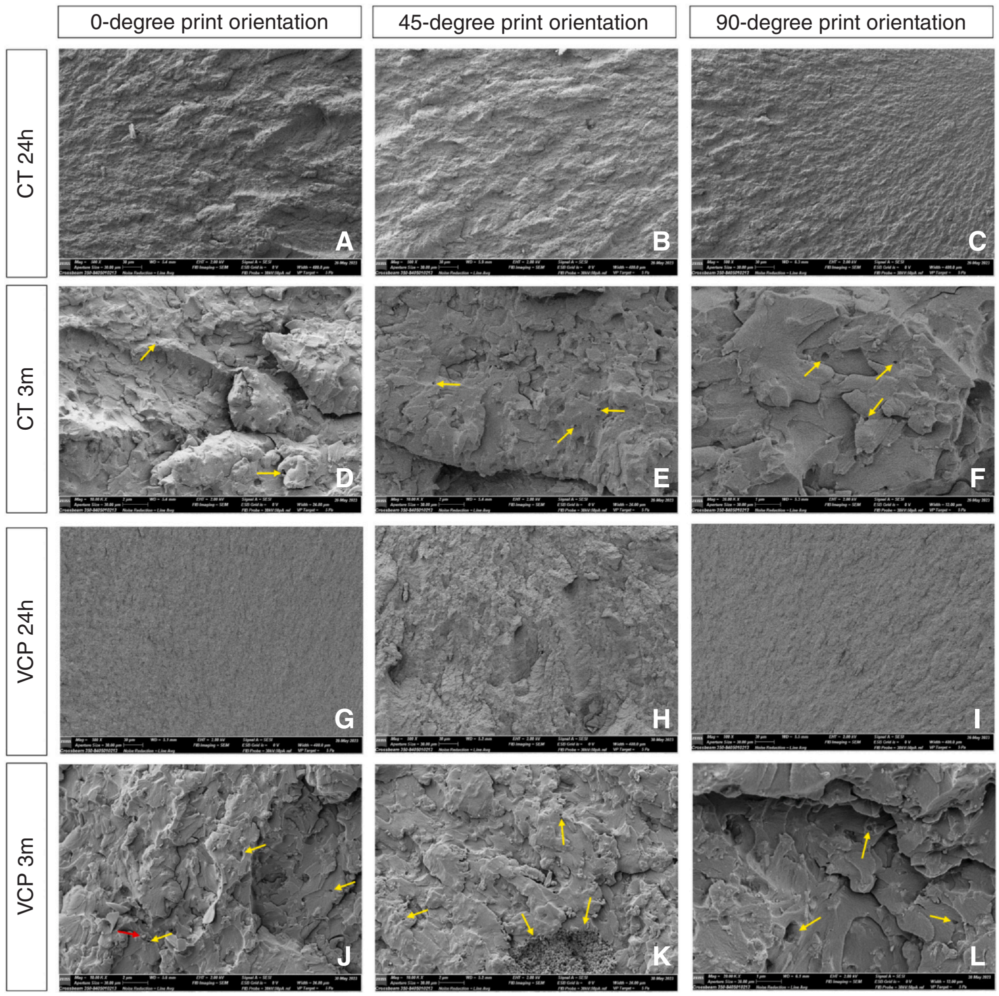


**Figure 5.** Fractured surface morphology of definitive 3-dimensionally printed materials with different print orientations at 24 h (original magnification ×500) and 3 months (original magnification ×20 000) in AS. *Yellow arrows* indicate spherical voids from filler detachment.

similar performance could be associated with increased filler particle size and reduced particle-matrix adhesion, causing the detachment and exfoliation of filler particles due to chemical degradation, which reduced the flexural strength.[49–51] The SEM images of GC and ND specimens (Fig. 6) showed this effect, while SEM images of DT images did not show any fillers, suggesting that the measured filler weight consists of only the pigments.

Monomers such as bisphenol A ethoxylate dimethacrylate (BisEMA), present in CT, have been reported to enhance the toughness and impact resistance of a resin because of their high molecular weight.[64] The high molecular weight allows the material to withstand bending forces without fracture and reduces water sorption because of the hydrophobic nature,[64] explaining the higher FS and FM observed in CT compared with interim 3D printed materials. GC contains a 50% to 75% monomer composition of urethane dimethacrylate (UDMA), which forms a flexible backbone with weak hydrogen bonding from the urethane groups, making it prone to water sorption and hydrolytic degradation, thereby reducing its strength.[52] In addition to the observed filler exfoliation in the SEM images, the composition explains why GC, despite having a higher filler load than ND and DT, exhibited the lowest FS after 3 months of aging. Monomers such as 2-hydroxyethyl methacrylate (HEMA) in ND absorb water because of their hydrophilic nature, leading to decreased FS and FM over time, as observed in this study and consistent with other findings.[19,22]

The variations observed among the 3D printed materials can also be attributed to the specific postpolymerization devices used. Studies have highlighted the significant impact of these devices and the duration of their use on the mechanical properties of dental resins, a relationship directly linked to the degree of conversion.[23,32,65] This study used 3 different postpolymerization devices as recommended by each material's manufacturer (Table 2). Generally, specimens postpolymerized in Ottoflash (CT, VCP) exhibited

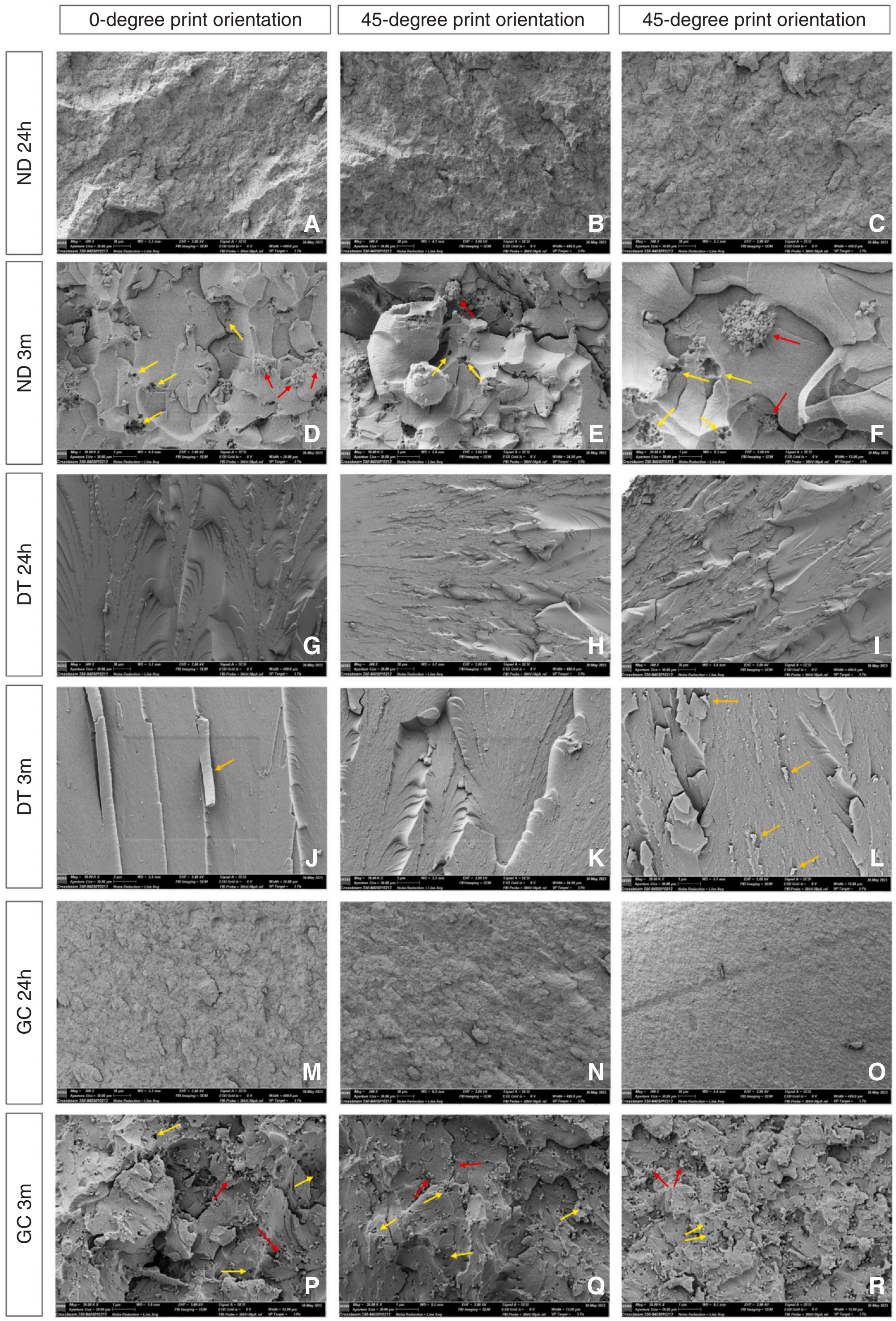


**Figure 6.** Fractured surface morphology of interim 3-dimensionally printed materials with different print orientations at 24 h (original magnification ×500) and at 3 months (original magnification ×10 000 to ×20 000) in AS. *Yellow arrows* indicate spherical voids from filler detachment. *Red arrows* indicate filler particles and clusters. *Orange arrows* indicate signs of peeling.

higher FS than those postpolymerized in Form Cure (ND) and Cara Print LED Cure (DT). This finding was consistent with previous research indicating that specimens postpolymerized in Ottoflash exhibited superior fracture load,[20] elastic modulus, and degree of conversion.[21] The broad light spectrum and concentrated flashes of Ottoflash likely resulted in higher energy and temperature, expediting polymerization.[66]

Reymus et al[67] reported that light emitting diode (LED) postpolymerization devices yielded inferior mechanical properties compared with Ottoflash and UV light devices, likely because of an inadequate degree of conversion from the LED light sources. In this study, DT, the only material postpolymerized with the LED unit, showed the lowest FS and FM, possibly because of the lack of fillers or inadequate postpolymerization time or a mismatch between the photoinitiator system and the LED wavelength, leading to incomplete polymerization.[68]

Regarding artificial aging, FS and FM measurements in DW were initially higher than those in AS. However, after 3 months, no significant difference in FS between DW and AS was observed ($P$>.05), suggesting that AS is a more deteriorating medium for evaluating resin materials than DW over a short period. Over a longer aging period, resin materials reacted similarly to both DW and AS. Thus, DW and AS have similar long-term effects, consistent with another study.[69] The greater impact of AS is because of its lower pH (5.3) compared with DW (6.5), which can leach residual monomers and damage inorganic fillers, reducing the FS.[70] Therefore, comparisons between milled and 3D printed materials were conducted only in AS.

The behavior of the 90-degree specimens varied over time and was material specific. ND showed a decline in FS and FM, while GC and DT increased after 3 months compared with 24 hours. The FS of VCP and CT in AS remained relatively unaffected by aging. The decline in mechanical properties can be attributed to solvent penetration into the resin matrix, causing swelling and plasticization, filler dislodgment, and the release of nonreacted components, which reduce the mechanical properties.[19,54,71] Multiple voids resulting from filler dislodgment are visible in the SEM images after 3 months (Fig. 6). Conversely, a warm storage medium might induce additional crosslinking, increasing the mechanical properties.[20,53]

The FS of GC and DT increased after 3 months compared with 24 hours but decreased compared with 1 month, showing the impact of extended storage time on material properties. These changes are linked to water absorption, which is influenced by the resin matrix composition and filler loading.[52,71] Despite this increase, their mean FS remained the lowest among the tested materials, similar to ND. The SEM images of aged GC and ND support these low measurements, showing voids from filler detachment, while DT showed peeling, possibly due to its methacrylate monomer composition and lack of fillers.

All 3D printed materials demonstrated lower FS and FM compared with the milled LU, which was expected considering it has the highest filler load (74%). LU incorporates nanoclusters of nonaggregated, nonagglomerated silica and zirconia nanoparticles, which have been linked to a higher elastic modulus than spherical fillers.[45,72,73] Additionally, the monomer composition of LU, which includes bisphenol A glycerolate dimethacrylate (Bis-GMA), triethylene glycol dimethacrylate (TEGDMA), Bis-EMA, and UDMA, forms a densely crosslinked network, enhancing durability and minimizing softening.[74] In contrast, 3D printed materials face viscosity constraints that hinder filler incorporation, leading to lower FS and FM[49,75,76] and explaining the comparatively lower FS and FM observed in 3D printed materials compared with milled composite resin LU, similar to the findings of Prause et al.[38] Other studies comparing milled definitive crowns with 3D printed definitive crowns using VCP or CT reported similar or lower fracture resistance for 3D printed crowns.[13,15,37,39,41] However, direct comparisons are challenging because of variations in specimen geometry, printing parameters, and control materials.

TC exhibited FS similar to both definitive and interim 3D printed materials despite lacking fillers while maintaining a FM similar to that of interim ones. This high FS may be because of the high-pressure and high-temperature polymerization process in an industrial setting, which enhances the degree of conversion and mechanical properties, resulting in a more robust polymer network.[67,77–79] The higher FS of milled PMMA materials compared with 3D printed ones for interim restorations has been reported,[17,24,43] though another study[33] reported no significant difference.

Based on the current findings, all tested materials printed at a 90-degree orientation met the ISO 4049 standard specifications, and their performance remained largely unaffected after storage in media simulating their environment. Limitations of this study included the in vitro design that only simulated the chemical aspect of aging and therefore may not have accurately predicted clinical performance. Consequently, 3D printed definitive resins might not perform as well clinically in the long term as milled FDPs. Future investigations should assess the impact of aging induced by mastication, examine material stability under varying temperature conditions, and explore the effects of different solvents encountered in the oral environment. Using specimen shapes that closely resemble those in clinical applications would offer a more accurate representation of material performance in clinical scenarios. The effects of printing specimens horizontally but with the force applied on the edge should be investigated.

## CONCLUSIONS

Based on the findings of this in vitro study, the following conclusions were drawn:

1. The 90-degree print orientation produced specimens with higher flexural strength than 0-degree and 45-degree print orientations.
2. 3D printed resin CT recommended for definitive restorations displayed higher FS compared with

VCP and those intended for interim use after 3 months of aging.

3. Milled composite resin LU exhibited higher FS and FM than 3D printed resins, while milled PMMA resin TC had similar FS and FM to 3D printed resin.
4. AS was a more deteriorating medium initially but, after 3 months, DW and AS had similar effects, while the effect of aging time was material specific.

## REFERENCES

1. Shim JS, Kim J-E, Jeong SH, et al. Printing accuracy, mechanical properties, surface characteristics, and microbial adhesion of 3D-printed resins with various printing orientations. *J Prosthet Dent*. 2020;124:468–475.
2. Kessler A, Reymus M, Hickel R, Kunzelmann K-H. Three-body wear of 3D printed temporary materials. *Dent Mater*. 2019;35:1805–1812.
3. Della Bona A, Cantelli V, Britto VT, et al. 3D printing restorative materials using a stereolithographic technique: A systematic review. *Dent Mater*. 2021;37:336–350.
4. Stansbury JW, Idacavage MJ. 3D printing with polymers: Challenges among expanding options and opportunities. *Dent Mater*. 2016;32:54–64.
5. Ligon SC, Liska R, Stampfl Jr, et al. Polymers for 3D printing and customized additive manufacturing. *Chem Rev*. 2017;117:10212–10290.
6. Arefin AM, Khatri NR, Kulkarni N, Egan PF. Polymer 3D printing review: Materials, process, and design strategies for medical applications. *Polymers (Basel)*. 2021;13:1499.
7. Kessler A, Hickel R, Reymus M. 3D printing in dentistry—State of the art. *Oper Dent*. 2020;45:30–40.
8. Siripongpreda T, Hoven VP, Narupai B, Rodthongku N. Emerging 3D printing based on polymers and nanomaterial additives: Enhancement of properties and potential applications. *Eur Polym J*. 2023;184:111806.
9. Kessler A, Dosch M, Reymus M, Folwaczny M. Influence of 3D-printing method, resin material, and sterilization on the accuracy of virtually designed surgical implant guides. *J Prosthet Dent*. 2022;128:196–204.
10. Altarazi A, Haider J, Alhotan A, et al. Assessing the physical and mechanical properties of 3D printed acrylic material for denture base application. *Dent Mater*. 2022;38:1841–1854.
11. Goodacre BJ, Goodacre CJ. Additive manufacturing for complete denture fabrication: A narrative review. *J Prosthodont*. 2022;31:47–51.
12. Prpic V, Spehar F, Stajdohar D, et al. Mechanical properties of 3D-printed occlusal splint materials. *Dent J (Basel)*. 2023;11:199.
13. Atria PJ, Bordin D, Marti F, et al. 3D-printed resins for provisional dental restorations: Comparison of mechanical and biological properties. *J Esthet Restor Dent*. 2022;34:804–815.
14. Revilla-León M, Supaphakorn A, Barmak AB, et al. Influence of print orientation on the intaglio surface accuracy (trueness and precision) of tilting stereolithography definitive resin-ceramic crowns. *J Prosthet Dent* 2023.
15. Donmez MB, Okutan Y. Marginal gap and fracture resistance of implant-supported 3D-printed definitive composite crowns: An in vitro study. *J Dent*. 2022;124:104216.
16. Jain S, Sayed ME, Shetty M, et al. Physical and mechanical properties of 3d-printed provisional crowns and fixed dental prosthesis resins compared to cad/cam milled and conventional provisional resins: A systematic review and meta-analysis. *Polymers (Basel)*. 2022;14:2691.
17. Nold J, Wesemann C, Rieg L, et al. Does printing orientation matter? In-vitro fracture strength of temporary fixed dental prostheses after a 1-year simulation in the artificial mouth. *Materials ((Basel))*. 2021;14:259.
18. Unkovskiy A, Bui PH-B, Schille C, et al. Objects build orientation, positioning, and curing influence dimensional accuracy and flexural properties of stereolithographically printed resin. *Dent Mater*. 2018;34:e324–e333.
19. Kessler A, Hickel R, Ilie N. In vitro investigation of the influence of printing direction on the flexural strength, flexural modulus and fractographic analysis of 3D-printed temporary materials. *Dent Mater J*. 2021;40:641–649.
20. Reymus M, Fabritius R, Keßler A, et al. Fracture load of 3D-printed fixed dental prostheses compared with milled and conventionally fabricated ones: The impact of resin material, build direction, post-curing, and artificial aging—An in vitro study. *Clin Oral Investig*. 2020;24:701–710.
21. Mayinger F, Reymus M, Liebermann A, et al. Impact of polymerization and storage on the degree of conversion and mechanical properties of veneering resin composites. *Dent Mater J*. 2021;40:487–497.
22. Scherer MD, Husain NA-H, Barmak AB, et al. Influence of postprocessing rinsing solutions and duration on flexural strength of aged and nonaged additively manufactured interim dental material. *J Prosthet Dent*. 2024;131:959–968.
23. Soto-Montero J, de Castro EF, Romano BdC, et al. Color alterations, flexural strength, and microhardness of 3D printed resins for fixed provisional restoration using different post-curing times. *Dent Mater*. 2022;38:1271–1282.
24. de Castro EF, Nima G, Rueggeberg FA, Giannini M. Effect of build orientation in accuracy, flexural modulus, flexural strength, and microhardness of 3D-Printed resins for provisional restorations. *J Mech Behav Biomed Mater*. 2022;136:105479.
25. Turksayar AAD, Donmez MB, Olcay EO, et al. Effect of printing orientation on the fracture strength of additively manufactured 3-unit interim fixed dental prostheses after aging. *J Dent*. 2022;124:104155.
26. Tahir N, Abduo J. An in vitro evaluation of the effect of 3d printing orientation on the accuracy of implant surgical templates fabricated by desktop printer. *J Prosthodont*. 2022;31:791–798.
27. Väyrynen VO, Tanner J, Vallittu PK. The anisotropicity of the flexural properties of an occlusal device material processed by stereolithography. *J Prosthet Dent*. 2016;116:811–817.
28. Zohdi N, Yang R. Material anisotropy in additively manufactured polymers and polymer composites: A review. *Polymers (Basel)*. 2021;13:3368.
29. Alharbi N, Osman R, Wismeijer D. Effects of build direction on the mechanical properties of 3D-printed complete coverage interim dental restorations. *J Prosthet Dent*. 2016;115:760–767.
30. Štaffová M, Ondreáš F, Svatík J, et al. 3D printing and post-curing optimization of photopolymerized structures: Basic concepts and effective tools for improved thermomechanical properties. *Polym Test*. 2022;108:107499.
31. Al Wadei MHD, Sayed ME, Jain S, et al. Marginal adaptation and internal fit of 3D-printed provisional crowns and fixed dental prosthesis resins compared to CAD/CAM-milled and conventional provisional resins: A systematic review and meta-analysis. *Coatings*. 2022;12:1777.
32. Chang J, Choi Y, Moon W, Chung SH. Impact of postpolymerization devices and locations on the color, translucency, and mechanical properties of 3D-printed interim resin materials. *J Prosthet Dent* 2022.
33. Park S-M, Park J-M, Kim S-K, et al. Flexural strength of 3D-printing resin materials for provisional fixed dental prostheses. *Materials (Basel)*. 2020;13:3970.
34. Derban P, Negrea R, Rominu M, Marsavina L. Influence of the printing angle and load direction on flexure strength in 3D printed materials for provisional dental restorations. *Materials (Basel)*. 2021;14:3376.
35. Tahayeri A, Morgan M, Fugolin AP, et al. 3D printed versus conventionally cured provisional crown and bridge dental materials. *Dent Mater*. 2018;34:192–200.
36. Grzebieluch W, Kowalewski P, Grygier D, et al. Printable and machinable dental restorative composites for cad/cam application—Comparison of mechanical properties, fractographic, texture and fractal dimension analysis. *Materials (Basel)*. 2021;14:4919.
37. Diken Türksayar AA, Demirel M, Donmez MB, et al. Comparison of wear and fracture resistance of additively and subtractively manufactured screw-retained, implant-supported crowns. *J Prosthet Dent*. 2024;132:154–164.
38. Prause E, Malgaj T, Kocjan A, et al. Mechanical properties of 3D-printed and milled composite resins for definitive restorations: An in vitro comparison of initial strength and fatigue behavior. *J Esthet Restor Dent* 2023.
39. Arafa A, Ziada A. Marginal adaptability and fracture resistance of endodontically treated premolars restored with 3D printed and milled endo-crowns. *Egypt Dent J*. 2023;69:2137–2152.
40. Schulz A-C, Othman A, Ströbele D-A, et al. Fracture strength test of digitally produced ceramic-filled and unfilled dental resin restorations via 3d printing: An in vitro study. *J Clin Exp Dent*. 2023;15:e118.
41. Suksuphan P, Krajangta N, Didron PP, et al. Marginal adaptation and fracture resistance of milled and 3D-printed CAD/CAM hybrid dental crown materials with various occlusal thicknesses. *J Prosthodont Res*. 2023;68:326–335.
42. Çakmak G, Donmez MB, de Paula MS, et al. Surface roughness, optical properties, and microhardness of additively and subtractively manufactured CAD-CAM materials after brushing and coffee thermal cycling. *J Prosthodont* 2023.
43. Digholkar S, Madhav V, Palaskar J. Evaluation of the flexural strength and microhardness of provisional crown and bridge materials fabricated by different methods. *J Indian Prosthodont Soc*. 2016;16:328.
44. Gonçalves F, Kawano Y, Pfeifer C, et al. Influence of BisGMA, TEGDMA, and BisEMA contents on viscosity, conversion, and flexural strength of experimental resins and composites. *Eur J Oral Sci*. 2009;117:442–446.
45. Kim K-H, Ong JL, Okuno O. The effect of filler loading and morphology on the mechanical properties of contemporary composites. *J Prosthet Dent*. 2002;87:642–649.
46. Leprince J, Palin W, Mullier T, et al. Investigating filler morphology and mechanical properties of new low-shrinkage resin composite types. *J Oral Rehabil*. 2010;37:364–376.
47. Schwartz J, Söderholm KJ. Effects of filler size, water, and alcohol on hardness and laboratory wear of dental composites. *Acta Odontol Scand*. 2004;62:102–106.

48. Barszczewska-Rybarek IM. Structure-property relationships in dimethacrylate networks based on Bis-GMA, UDMA and TEGDMA. *Dent Mater*. 2009;25:1082–1089.
49. Mayer J, Reymus M, Mayinger F, et al. Temporary 3D-printed fixed dental prosthesis materials: Impact of postprinting cleaning methods on degree of conversion and surface and mechanical properties. *Int J Prosthodont*. 2021;34.
50. Rodríguez HA, Kriven WM, Casanova H. Development of mechanical properties in dental resin composite: Effect of filler size and filler aggregation state. *Mater Sci Eng C Mater Biol Appl*. 2019;101:274–282.
51. Fu S-Y, Feng X-Q, Lauke B, Mai Y-W. Effects of particle size, particle/matrix interface adhesion and particle loading on mechanical properties of particulate–polymer composites. *Compos B Eng*. 2008;39:933–961.
52. Ferracane JL. Hygroscopic and hydrolytic effects in dental polymer networks. *Dent Mater*. 2006;22:211–222.
53. Yap A, Chandra S, Chungo S, Lim C. Changes in flexural properties of composite restoratives after aging in water. *Oper Dent*. 2002;27:468–474.
54. Berli C, Thieringer FM, Sharma N, et al. Comparing the mechanical properties of pressed, milled, and 3D-printed resins for occlusal devices. *J Prosthet Dent*. 2020;124:780–786.
55. Standardization I. ISO 4049: Dentistry—Polymer-Based Restorative Materials. International Organization for Standardization (ISO),; 2019.
56. ISO E. 1172: 1999; Textile-Glass-Reinforced Plastics—Prepregs, Moulding Compounds and Laminates—Determination of the Textile-Glass and Mineral-Filler Content Using Calcination Methods (ISO 1172: 2023).
57. Hampe R, Lümkemann N, Sener B, Stawarczyk B. The effect of artificial aging on Martens hardness and indentation modulus of different dental CAD/CAM restorative materials. *J Mech Behav Biomed Mater*. 2018;86:191–198.
58. Correr GM, Bruschi Alonso RC, Baratto-Filho F, et al. In vitro long-term degradation of aesthetic restorative materials in food-simulating media. *Acta Odontol Scand*. 2012;70:101–108.
59. Fusayama T, Katayori T, Nomoto S. Corrosion of gold and amalgam placed in contact with each other. *J Dent Res*. 1963;42:1183–1197.
60. El Mallakh B, Sarkar N. Fluoride release from glass-ionomer cements in de-ionized water and artificial saliva. *Dent Mater*. 1990;6:118–122.
61. Ilie N, Hilton T, Heintze S, et al. Academy of dental materials guidance—Resin composites: Part I—Mechanical properties. *Dent Mater*. 2017;33:880–894.
62. No IS. 10477. Dentistry—Polymer-based crown and veneering materials. Geneva, Switzerland: International Organization for Standardization,; 2020.
63. Ikejima I, Nomoto R, McCabe JF. Shear punch strength and flexural strength of model composites with varying filler volume fraction, particle size and silanation. *Dent Mater*. 2003;19:206–211.
64. Gajewski VE, Pfeifer CS, Fróes-Salgado NR, et al. Monomers used in resin composites: Degree of conversion, mechanical properties and water sorption/solubility. *Braz Dent J*. 2012;23:508–514.
65. Silva NR, Moreira FGdG, Cabral ABdC, et al. Influence of the postpolymerization type and time on the flexural strength and dimensional stability of 3D-printed interim resins. *J Prosthet Dent*. 2023;130. 796.e1–.e8.
66. Rizzante FA, Magão P, Moura G, et al. Can postpolymerization for 3D-printed interim restorations be improved? *J Prosthet Dent*. 2022;128. 1102.e1–.e5.
67. Reymus M, Stawarczyk B. In vitro study on the influence of postpolymerization and aging on the Martens parameters of 3D-printed occlusal devices. *J Prosthet Dent*. 2021;125:817–823.
68. Kowalska A, Sokolowski J, Bociong K. The photoinitiators used in resin based dental composite—A review and future perspectives. *Polymers (Basel)*. 2021;13:470.
69. Alamoush RA, Sung R, Satterthwaite JD, Silikas N. The effect of different storage media on the monomer elution and hardness of CAD/CAM composite blocks. *Dent Mater*. 2021;37:1202–1213.
70. Alhotan A, Raszewski Z, Alamoush RA, et al. Influence of storing composite filling materials in a low-pH artificial saliva on their mechanical properties—An in vitro study. *J Funct BioMater*. 2023;14:328.
71. Grzebieluch W, Kowalewski P, Sopel M, Mikulewicz M. Influence of artificial aging on mechanical properties of six resin composite blocks for CAD/CAM application. *Coatings*. 2022;12:837.
72. Yin R, Kim Y-K, Jang Y-S, et al. Comparative evaluation of the mechanical properties of CAD/CAM dental blocks. *Odontology*. 2019;107:360–367.
73. Masouras K, Silikas N, Watts DC. Correlation of filler content and elastic properties of resin-composites. *Dent Mater*. 2008;24:932–939.
74. Söderholm K-J, Zigan M, Ragan M, et al. Hydrolytic degradation of dental composites. *J Dent Res*. 1984;63:1248–1254.
75. Taormina G, Sciancalepore C, Messori M, Bondioli F. 3D printing processes for photocurable polymeric materials: Technologies, materials, and future trends. *J Appl Biomater Funct Mater*. 2018;16:151–160.
76. Lim B-S, Ferracane JL, Condon JR, Adey JD. Effect of filler fraction and filler surface treatment on wear of microfilled composites. *Dent Mater*. 2002;18:1–11.
77. Lauvahutanon S, Takahashi H, Shiozawa M, et al. Mechanical properties of composite resin blocks for CAD/CAM. *Dent Mater J*. 2014;33:705–710.
78. Nguyen JF, Migonney V, Ruse ND, Sadoun M. Resin composite blocks via high-pressure high-temperature polymerization. *Dent Mater*. 2012;28:529–534.
79. Balkenhol M, Mautner MC, Ferger P, Wöstmann B. Mechanical properties of provisional crown and bridge materials: Chemical-curing versus dual-curing systems. *J Dent*. 2008;36:15–20.

**Corresponding author:**
Dr Shaymaa Mudhaffer
Division of Dentistry
School of Medical Sciences
University of Manchester
Coupland Building 3
Oxford Road
Manchester, England M13 9PL
UNITED KINGDOM
Email: S.mudhaffer@Taibahu.edu.sa

**Acknowledgments**
The authors thank Hayley Andrews (Faculty of Science and Engineering, Manchester Metropolitan University, Manchester, England, United Kingdom) for their contribution to the experimental work on scanning electron microscopy.

**CRediT authorship contribution statement**
**Shaymaa Mudhaffer:** Conceptualisation, Methodology, Software, Formal analysis, Investigation, Resources, Data curation, Writing—original draft preparation, Visualisation, Funding acquisition. **Julfikar Haider:** Validation, Writing—review and editing, Supervision. **Julian Satterthwaite:** Methodology, Validation, Writing—review and editing, Supervision, Project administration. **Nick Silikas:** Validation, Writing—review and editing, Supervision, Project administration.


https://doi.org/10.1016/j.prosdent.2024.08.008